



## Validation of QuikSCAT wind vectors by dropwindsonde data from Dropwindsonde Observations for Typhoon Surveillance Near the Taiwan Region (DOTSTAR)

Kun-Hsuan Chou,<sup>1</sup> Chun-Chieh Wu,<sup>2</sup> Po-Hsiung Lin,<sup>2</sup> and Sharanya Majumdar<sup>3</sup>

Received 31 March 2009; revised 27 August 2009; accepted 15 September 2009; published 26 January 2010.

[1] The accuracy of 10 m wind vectors derived from the QuikSCAT satellite near tropical cyclones is validated against soundings from 457 GPS dropwindsondes deployed by Dropwindsonde Observations for Typhoon Surveillance Near the Taiwan Region (DOTSTAR) during 2003–2007. To maximize the database, the surface to 40 m wind speed in the dropwindsondes is averaged and interpolated to the 10 m wind speed by linear regression. After removing rain-flagged data, the root-mean-square differences between QuikSCAT and dropwindsonde data were  $2.6 \text{ m s}^{-1}$  or 18% (wind speed) and  $17^\circ$  (wind direction) on the basis of 896 matching samples. Further analyses also indicate that the QuikSCAT data slightly underestimates the wind speed of medium-wind regime (between 10 and  $17.2 \text{ m s}^{-1}$ ) and possesses some clockwise directional bias in the high-wind regime (above  $17.2 \text{ m s}^{-1}$ ). In summary, this study suggests that the QuikSCAT wind vectors below tropical storm wind strength ( $17.2 \text{ m s}^{-1}$ ) are accurate enough for forecasters to determine the critical wind radius of 34 knot wind, while a new error bound of the QuikSCAT wind estimate in high-wind regimes near tropical cyclones is suggested to be set at about  $4 \text{ m s}^{-1}$ .

**Citation:** Chou, K.-H., C.-C. Wu, P.-H. Lin, and S. Majumdar (2010), Validation of QuikSCAT wind vectors by dropwindsonde data from Dropwindsonde Observations for Typhoon Surveillance Near the Taiwan Region (DOTSTAR), *J. Geophys. Res.*, 115, D02109, doi:10.1029/2009JD012131.

### 1. Introduction

[2] Given the paucity of routine in situ wind observations at the ocean surface with wide spatial coverage, ocean surface vector winds measured by spaceborne scatterometers have become tremendously useful for marine analysis and forecasting [Atlas *et al.*, 2001; Chelton *et al.*, 2006]. The leading example to date has been SeaWinds on board NASA's Quick Scatterometer (QuikSCAT), which was launched in 1999. Via backscatter values sampled from two microwave "pencil-beams," values of 10 m wind speed and direction at every point in a 1800 km wide swath are derived at 25 km resolution, subject to a sufficient lack of contamination of the beam by heavy rain (J. N. Huddleston and B. W. Stiles, Multidimensional Histogram (MUDH) rain flag product description (version 3.0), Jet Propulsion Laboratory, Pasadena, California, 2000, available at ftp://podaac.jpl.nasa.gov/quikscat/qscat\_doc.html). These wind fields derived from QuikSCAT have proven to be important

to NOAA's Ocean Prediction Center in the issuance of marine warnings, and specifically their ability to consistently observe or infer the intensity and areal extent of winds of hurricane force ( $32.9 \text{ m s}^{-1}$ ) in extratropical cyclones and marine weather over the open ocean [Von Ahn *et al.*, 2006]. Additionally, the utility of assimilating QuikSCAT data into global numerical weather prediction models has been demonstrated by Atlas *et al.* [2001].

[3] Several studies have been performed to evaluate the accuracy of scatterometer winds against surface buoy data. Freilich and Dunbar [1999] compared winds from NSCAT, the predecessor to QuikSCAT, with those measured by 43 buoys offshore of the eastern and western United States. They found the root-mean-square (rms) differences in wind speed and direction to be  $1.3 \text{ m s}^{-1}$  and  $17^\circ$ , respectively. In a comparison between QuikSCAT winds and nearshore and offshore buoy data, Pickett *et al.* [2003] showed that the wind differences nearshore were larger than those offshore, with the RMS differences in wind speed and direction decreasing from  $1.3 \text{ m s}^{-1}$  and  $26^\circ$  nearshore to  $1.0 \text{ m s}^{-1}$  and  $15^\circ$  offshore. These values are similar to those obtained by Ebuchi *et al.* [2002], who found that the RMS differences between QuikSCAT and offshore buoy data were  $1.0 \text{ m s}^{-1}$  and  $20^\circ$ . These previous studies demonstrated that the RMS differences between scatterometer and buoy data lied within the satellite's design specifications for wind speed ( $\pm 2 \text{ m s}^{-1}$ ) and close to that for direction ( $\pm 20^\circ$ ) [Pickett *et al.*, 2003].

<sup>1</sup>Department of Atmospheric Sciences, Chinese Culture University, Taipei, Taiwan.

<sup>2</sup>Department of Atmospheric Sciences, National Taiwan University, Taipei, Taiwan.

<sup>3</sup>Division of Meteorology and Physical Oceanography, Rosenstiel School of Marine and Atmospheric Science, University of Miami, Miami, Florida, USA.

[4] Though studies such as the above have demonstrated the accuracy of winds derived from QuikSCAT in a variety of applications, their accuracy in heavily precipitating regimes such as tropical cyclones (TCs) is severely compromised owing to the contamination of backscatter. Mindful of this reservation, tropical analysts and forecasters routinely use QuikSCAT data in their preparation of surface wind analyses in the environment of TCs [Brennan *et al.*, 2009]. For example, the U.S. National Hurricane Center regularly prepares manual analyses of directional ambiguities to detect whether a closed surface circulation exists in a developing TC, and their Tropical Analysis and Forecast Branch uses QuikSCAT data to issue wind warnings associated with fronts, cyclones, and gap wind events. However, the effects of rain, resolution and signal saturation severely limit the ability of operational forecasters to determine the wind speed of the TC. An additional operational use of the QuikSCAT data, most relevant to this paper, is the detection of the radius of tropical storm force winds ( $17.2 \text{ m s}^{-1}$ ), which is important both for wind warnings and for classification of whether a TC has reached tropical storm strength. While Brennan *et al.* [2009] have stated that “wind radii information from QuikSCAT is particularly valuable for TCs not sampled for aircraft reconnaissance,” the comparisons between scatterometer winds and in situ data in the environment of the TC are rare. The first study of scatterometer observations and validation by in situ observations over TCs was accomplished by SEASAT-A Satellite Scatterometer (SASS) for use in determination of TC gale force wind radii in the work of Hawkins and Black [1983] and Black *et al.* [1985]. They first investigated the SASS wind statistics near the storm center by fifty matching samples of SASS derived wind speeds with surface truth values. The RMS error of non-rain-contaminated wind was  $0.8 \text{ m s}^{-1}$  for wind speed and  $11^\circ$  for wind direction, and RMS error of rain contaminated wind indicated larger errors of  $1.6 \text{ m s}^{-1}$  and  $18.5^\circ$ . It is worth noting that the wind speeds in the storm areas are often considerably stronger than those in the aforementioned papers on QuikSCAT data comparison, and there is the additional risk of rain contamination from rainbands.

[5] In this paper, we perform a comparison between QuikSCAT winds and equivalent wind observations from the Global Positioning System (GPS) dropwindsonde, for TCs over the northwest Pacific Ocean. The tropospheric soundings obtained from Dropwindsonde Observations for Typhoon Surveillance Near the Taiwan Region (DOTSTAR) surveillance aircraft missions provide a unique data set for the validation and calibration of remotely sensed data for TCs in this region [Wu *et al.*, 2005, 2007a, 2007b; Chou and Wu, 2008]. An improved characterization of the accuracy of QuikSCAT winds in the environment of TCs would lead to better operational analyses of tropical storm force winds, higher-quality reanalysis fields used routinely in TC research, and improved initial conditions in forecast models that yield better forecasts of TC track and intensity. The results will also serve to provide a benchmark upon which data from future generations of scatterometers are expected to improve, in the environment of TCs.

[6] In section 2, we review the data and techniques used to increase the size and quality of the sample. Results for different wind regimes are provided in section 3, followed

by a discussion and conclusions in sections 4 and 5, respectively.

## 2. Data

### 2.1. QuikSCAT

[7] The QuikSCAT data used for this study are taken from the 2003–2007 observations archived at Remote Sensing Systems (<http://www.ssmi.com>). The 13.4 GHz Ku-band scatterometer transmits two microwave “pencil-beam” pulses with slightly different angles of incidence, which are scanned in a circle about the nadir. The back-scattered power from ocean surface capillary waves is then converted into wind vectors at 10 m height, assuming a neutrally stable atmosphere [Liu and Tang, 1996]. The wind data have been retrieved by the Ku-2001 model function, which is a distant relative of the NSCAT-1 model function developed for NSCAT [Wentz and Smith, 1999]. In addition to the geophysical model function, their wind data processing uses contemporaneous microwave radiometer measurements by three Special Sensor Microwave Imagers and the Tropical Rainfall Measuring Mission Microwave Imager for rain flagging and sea ice detection. For further details of the QuikSCAT platform and wind retrieval techniques, the reader is referred to the work of Hoffman and Leidner [2005].

[8] Rain is a well-known problem affecting the Ku-band scatterometers, and it tends to result in erroneous cross track vectors and/or unrealistically high speeds. Recently, a simple wind/rain backscatter model is used with collocated precipitation radar data to evaluate the effect of rain on QuikSCAT scatterometers by Draper and Long [2004]. Using the wind/rain model, there is a threshold where wind speeds are high enough that rain impacts are negligible regardless of rain rate, and accurate retrievals can be made. Furthermore, a model for the effects of rain on scatterometer-derived winds has been proposed by Hilburn *et al.* [2006]. This model accounts for contamination, rain roughening of the sea surface, and volumetric backscatter. The error statistics of the rain-contaminated QuikSCAT data as verified against the nearby dropwindsonde data is also investigated and will be discussed in section 3.

### 2.2. GPS Dropwindsonde

[9] The National Center for Atmospheric Research (NCAR) Global Positioning System (GPS) dropwindsonde provided the first set of reliable wind measurements with abundant high-wind records near the sea surface. The dropwindsonde has four main components: the pressure, temperature, humidity sensor module; the digital microprocessor circuitry; the GPS receiver module; and the 400 MHz transmitter. With a sampling rate of 2 Hz and a near-surface fall rate of  $11\text{--}12 \text{ m s}^{-1}$ , the vertical resolution of both the wind and thermodynamic observations from the dropwindsonde in the lower troposphere is approximately 5 m. The estimated typical measurement errors in the wind speed are  $0.5\text{--}2.0 \text{ m s}^{-1}$  [Hock and Franklin, 1999].

[10] The data set used for the validation in this study consists of 457 dropwindsonde atmospheric sounding profiles obtained during the 2003–07 seasons, during the 28 observation missions for 24 typhoons in DOTSTAR. Of the

457 profiles, most are deployed within 200–500 km from the center of the typhoon. The quality control of all dropwindsonde data is performed through the Atmospheric Sounding Processing Environment (Aspen) system origi-

nally designed by NCAR. The splash location of dropwindsonde is used for the validation in this study.

**2.3. Definition of M40: The Average Wind Between the Surface and 40 m**

[11] Although the GPS dropwindsonde has a sampling interval of 0.5 s, not all the dropwindsondes directly measure the 10 m wind ( $U_{10}$ ). In the data set used in this study, only 178 (39%) of the dropwindsondes recorded  $U_{10}$ . Thus, in order to obtain a larger sampling database, the surface to 40-m-averaged wind speed (M40) is calculated and interpolated to  $U_{10}$  by a regression fit that we describe here. The M40 is calculated if at least one valid wind between 0 and 40 m is available. As shown in Figure 1a, the calculation indicates that 357 dropwindsondes (78% of all dropwindsondes) are available for the M40 calculation, where the averaged number of sampling layers is 4.4 and the maximum number of sampling layers is 8. The RMS difference between each sample point and M40 for all 1581 samples is only  $0.6 \text{ m s}^{-1}$  (or roughly 5%), which means that the dropwindsonde measurements are quite stable when falling from 40 m to the surface (Figure 1a). The scatter diagram between the M40 and  $U_{10}$  (Figure 1b) indicates that the values of M40 match very well with  $U_{10}$ . The corresponding best fit regression line between the M40 and  $U_{10}$  values is given by  $U_{10-M40} = 0.977 * M40 + 0.056$ , with the correlation coefficient square ( $R^2$ ) of 0.996, where  $U_{10-M40}$  is the estimated 10 m wind based on the 357 GPS dropwindsondes. For the 178 dropwindsondes that directly measured  $U_{10}$ , the RMS difference in wind speed (direction) between  $U_{10-M40}$  and  $U_{10}$  is only  $0.3 \text{ m s}^{-1}$  ( $1.4^\circ$ ) (Figure 1c). The regression fits between the  $U_{10}$  and the averaged marine boundary layer wind (MBL, surface to 500-m-averaged wind [Franklin *et al.*, 2003]) and between  $U_{10}$  and surface to 150-m-averaged wind (M150) are also conducted in this study. It should be noted that the M150 calculation originated from the WL150 method [Franklin *et al.*, 2003; Uhlhorn *et al.*, 2007]. The WL150 is calculated on the basis of data at the lowest 150 m above 10 m, and is only valid if valid winds are obtained below about 350 m. In other words, the lowest level of WL150 is 10–160 m, and the highest is 200–350 m. The operational procedure at the National Hurricane Center in the United States is then to convert these values to  $U_{10}$  using an empirical function that depends upon the midheight of the 150 m layer. It should be noted that the reason for going to WL150 from original MBL wind estimate in TC is that in the near core the dropsondes frequently lost wind measurement below 150 m (loose locking on GPS signal due to low-level turbulence). This limitation of GPS dropsonde implies that M40 would not be so useful in eye wall of TC, but likely would be very useful elsewhere in TC, such as the dropwindsonde obser-

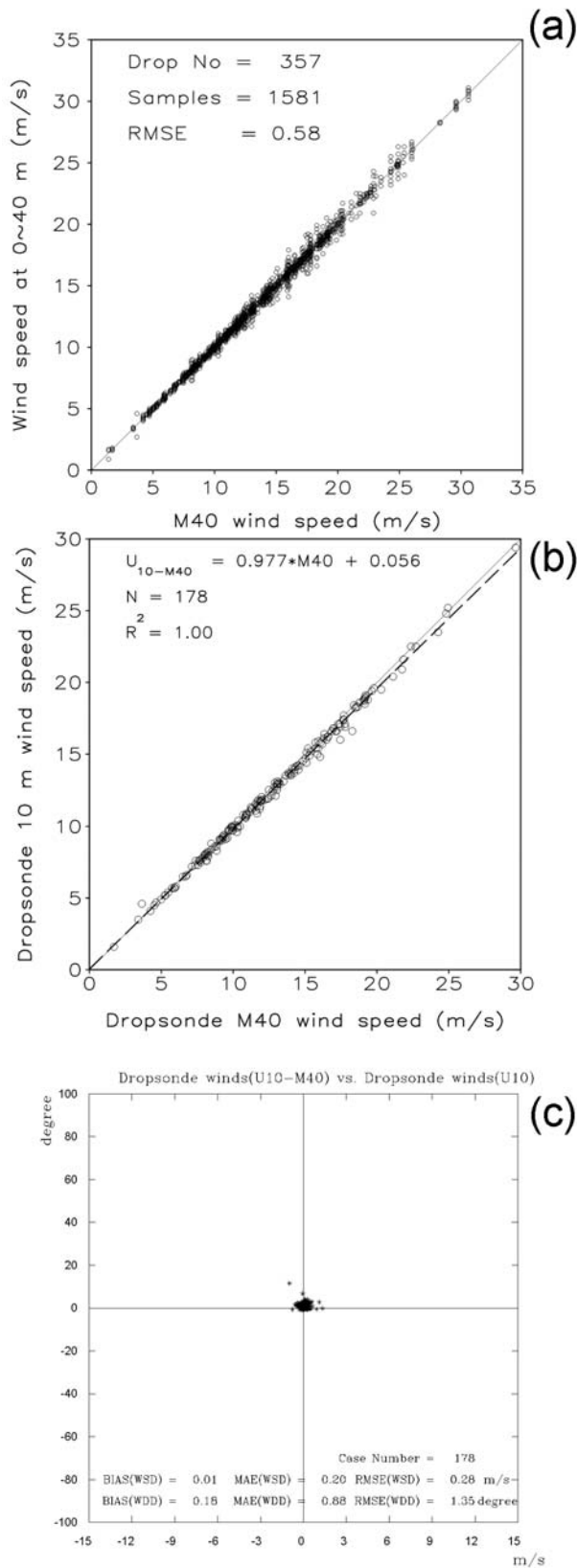


**Figure 1.** (a) Relationship between the averaged 0–40 m wind (M40) and GPS-measured wind speed at 0–40 m. (b) Scatter diagram of the wind speed with the linear regression fit line for the 10 m wind speed ( $U_{10}$ ) and the averaged 0–40 m wind (M40). (c) Scatter diagram of the wind speed and direction difference between the  $U_{10}$  and  $U_{10-M40}$  (the estimated 10 m wind by the M40 method).

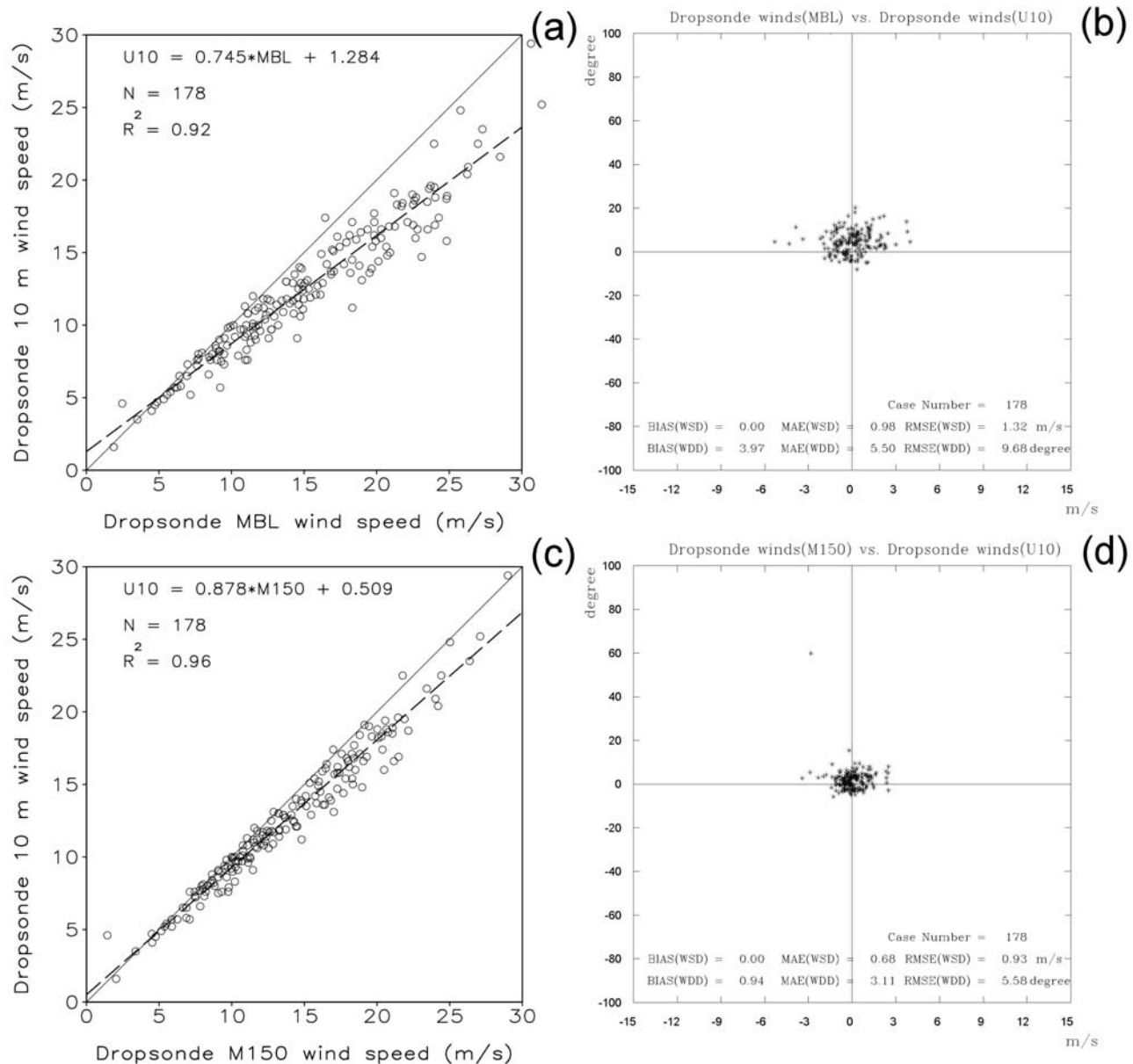


**Figure 2.** (a) Scatter diagram of the wind speed with the linear regression fit line for  $U_{10}$  and the MBL (surface to 500-m-averaged wind). (b) Scatter diagram of the wind speed and direction difference between  $U_{10}$  and  $U_{10-MBL}$  (the estimated 10 m wind by the MBL method). (c, d) Same as Figures 2a and 2b but for comparison between  $U_{10}$  and M150 (surface to 150-m-averaged wind).

variations from the DOTSTAR and NOAA G-IV surveillance missions.

[12] The calculation of M150 in this study is simplified as the surface to 150-m-averaged wind. The scatterplot and wind difference between the  $U_{10}$  and the marine boundary layer (MBL) and those between the  $U_{10}$  and the M150 are shown in Figure 2. The best fit regression line is  $U_{10-MBL} = 0.745 \cdot MBL + 1.284$  for comparison between  $U_{10}$  and MBL, and  $U_{10-M150} = 0.878 \cdot M150 + 0.509$  for comparison between  $U_{10}$  and M150. It is found that the  $R^2$  (0.921) between  $U_{10}$  and MBL and the  $R^2$  (0.961) between  $U_{10}$  and M150 are smaller than that (0.996) between  $U_{10}$  and M40. In addition, the RMS difference between  $U_{10-MBL}$  and  $U_{10}$

and those between  $U_{10-M150}$  and  $U_{10}$  increase to 1.3 and 0.9  $\text{m s}^{-1}$  in wind speed and 9.7° and 5.6° in wind direction. The cyclonic shift in wind direction in the MBL is likely related to the deeper boundary layer depth used for the calculation. Since the main motivation in this research is to validate the QuikSCAT wind vectors, we surmise that it is reasonable to use M40 method in this study to represent the 10 m wind for comparison.

#### 2.4. Time Matching of Observations

[13] The DOTSTAR GPS dropwindsondes are usually released between -3 h and 3 h of 0000 and 1200 UTC, within 10°–30°N and 115°–135°E. The QuikSCAT swath

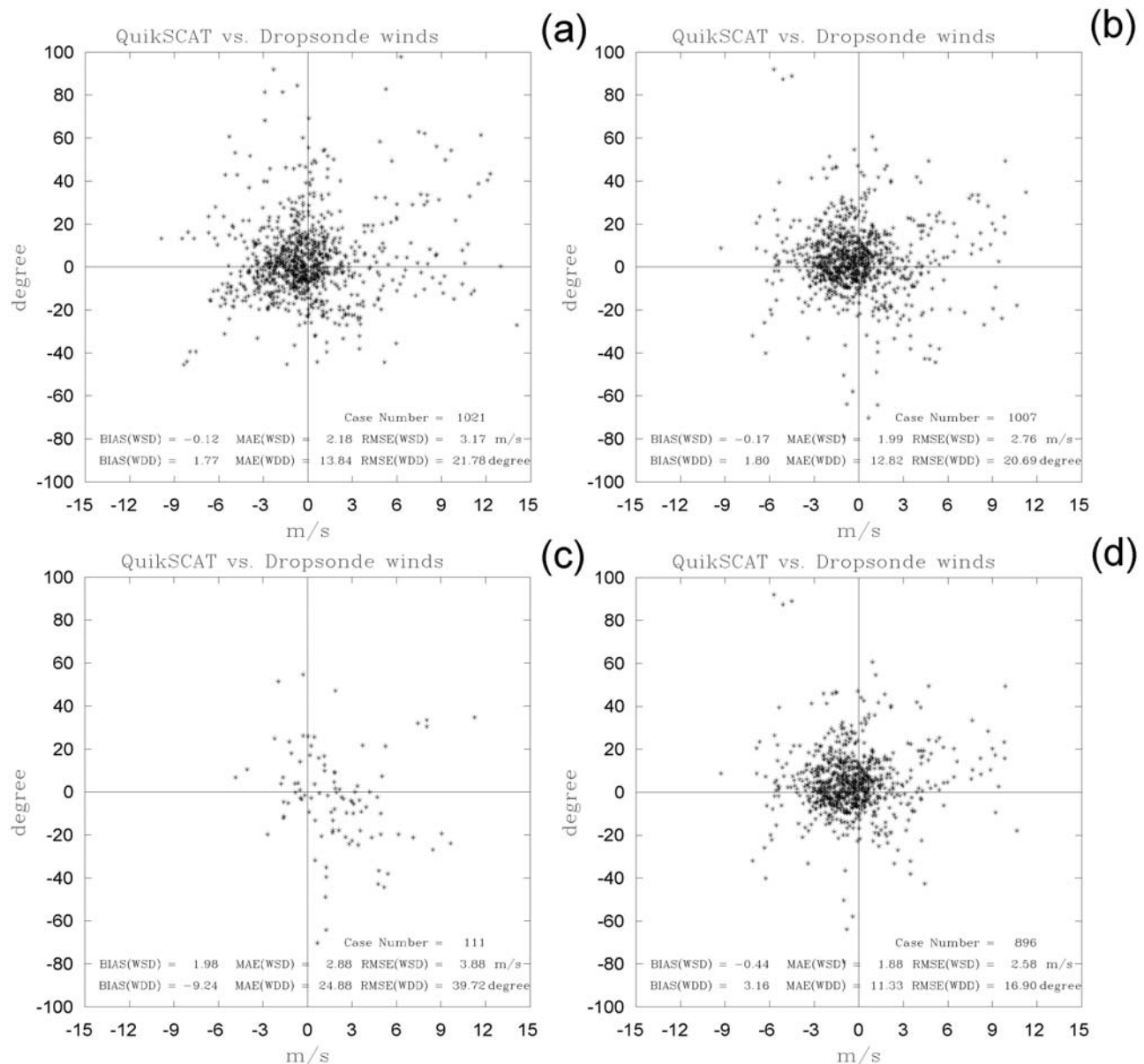


**Figure 3.** Scatter diagram of the wind speed and direction difference between the QuikSCAT surface wind and the estimated 10 m wind ( $U_{10-M40}$ ). (a) All QuikSCAT winds are verified with the dropwindsondes where the deployed locations are not modified. (b) Same as Figure 3a except that the dropwindsonde locations have been transformed to storm-relative coordinates. (c) Same as Figure 3b but for only the rain-flagged data. (d) Same as Figure 3c but for all the non-rain-flagged data.

passes this area at around 2200 and 1000 UTC. Thus, the data observed by the GPS dropwindsondes and QuikSCAT are usually not concurrent, and a method to adjust the data to match the times is necessary. The data are transformed in storm-relative coordinates at the time of the satellite overpass. The observations are compared when QuikSCAT and GPS dropwindsondes are within 0.25 degree radius of each other, or roughly one QuikSCAT footprint.

### 3. Results

#### 3.1. Comparison of Wind Speed and Direction

[14] Figure 3a shows the scatter diagram of the wind speed and direction difference between the QuikSCAT

surface wind and dropwindsonde estimated surface wind for all the matched samples, without employing the storm-relative coordinate transformation for the dropwindsondes (see section 2.4). On the basis of the calculation for 1021 available QuikSCAT-dropwindsonde matched samples, the mean speed difference is  $-0.1 \text{ m s}^{-1}$ , and the mean direction difference is  $1.8^\circ$  clockwise. Although the mean wind difference is small, the mean absolute difference and RMS wind differences are larger. The absolute mean and RMS difference of wind speed are  $2.2$  and  $3.2 \text{ m s}^{-1}$ , respectively, while those of wind direction are  $13.8^\circ$  and  $21.8^\circ$ , respectively. However, when the QuikSCAT data are compared with the dropwindsonde data in storm-relative

**Table 1.** Comparisons of Wind Speed and Direction Between QuikSCAT and Dropwindsonde Data<sup>a</sup>

QuikSCAT Data	Bias	Mean Absolute Difference	RMS Difference	Number of Matching Samples
<i>Non-Rain-Flagged Data</i>				
All	-0.4 (3.2)	1.9 (11.3)	2.6 (16.9)	896
V1: below 10 m s <sup>-1</sup>	0.1 (2.1)	0.9 (14.8)	1.2 (22.4)	182
V2: between 10 and 17.2 m s <sup>-1</sup>	-0.7 (2.1)	1.6 (9.6)	2.0 (12.8)	502
V3: above 17.2 m s <sup>-1</sup>	-0.4 (6.6)	3.3 (12.5)	4.1 (19.7)	212
<i>Rain-Flagged Data</i>				
All	2.0 (-9.2)	2.9 (24.9)	3.9 (39.7)	111
V1: below 10 m s <sup>-1</sup>	2.9 (-11.3)	3.0 (20.6)	3.9 (31.7)	50
V2: between 10 and 17.2 m s <sup>-1</sup>	1.6 (-7.9)	2.6 (28.0)	3.7 (45.6)	45
V3: above 17.2 m s <sup>-1</sup>	0.3 (-6.7)	3.2 (29.5)	4.5 (44.2)	16

<sup>a</sup>Wind speed is given in m s<sup>-1</sup>. Direction is given in degrees clockwise (value in parentheses).

coordinates, the scatter becomes slightly more concentrated toward the center, and the wind differences become smaller (Figure 3b). The RMS value of wind speed decreases from 3.2 to 2.8 m s<sup>-1</sup> and that of wind direction from 21.8° to 20.7° (Table 1). This result indicates that the conversion to storm-relative coordinates of the dropwindsonde locations increases the consistency between the dropwindsonde and QuikSCAT wind fields.

[15] For the subset of data points for which only rain-flagged data are included, the QuikSCAT rain-contaminated data have an obvious 2.0 m s<sup>-1</sup> and 9.2° counterclockwise bias (Figure 3c), indicating that the QuikSCAT winds are on average too strong, with a corresponding increased cyclonic component. The RMS differences are 3.9 m s<sup>-1</sup> for wind speed and 39.7° for wind direction. For the complementary subset in which all rain-flagged data are removed, Figure 3d illustrates that the RMS differences are smaller than when all data are included (2.6 m s<sup>-1</sup> for wind speed, 16.9° for wind direction). The wind error statistics of the rain- and non-rain-contaminated data of QuikSCAT calculated in this study is generally consistent with the findings of *Hawkins and Black* [1983], whose study contains limited (50) sample numbers.

### 3.2. Analysis of Different Wind Regimes

[16] Though the RMS value of wind direction calculated by this QuikSCAT-dropwindsonde comparison is similar to previous QuikSCAT-buoy comparisons [*Freilich and Dunbar*, 1999; *Ebuchi et al.*, 2002; *Pickett et al.*, 2003], the RMS difference in wind speed is slightly larger than their findings and exceeds the satellite's design specifications for wind speed ( $\pm 2$  m s<sup>-1</sup>). To examine the reason for these increased differences, the comparison is now stratified by different dropwindsonde estimated surface wind speeds.

[17] Figure 4 shows the QuikSCAT-dropwindsonde comparison for three different wind speed regimes: below 10 m s<sup>-1</sup> (V1), between 10 and 17.2 m s<sup>-1</sup> (V2), and above 17.2 m s<sup>-1</sup> (V3), classified by the magnitude of  $U_{10-M40}$ . For the rain-contaminated-data-only subset (Figures 4a, 4c, and 4e), although the sample amounts are fewer, the aforementioned wind speed bias mainly occurs at lower wind speeds, and the counterclockwise bias appears in all regimes.

[18] For the rain-flagged-data-removed subset (Figures 4b, 4d, and 4f), the scatter is more widespread in the regime of strongest winds (Figure 4f), with higher RMS values for both wind speed and direction. The RMS differences in wind direction are within the instrument design specifications

for wind direction ( $\pm 20^\circ$  [*Pickett et al.*, 2003]) in the two regimes of higher wind, but slightly outside the specifications for wind speeds below 10 m s<sup>-1</sup>. This large wind direction error for low winds is consistent with the findings of *Pickett et al.* [2003]. Furthermore, a systematic clockwise bias ( $\sim 7^\circ$ ) of wind direction can be found in locations of high wind (Figure 4f). Statistical examination by the paired test with two-sided distribution for the wind direction of QuikSCAT and dropwindsonde are calculated. The result indicates that the bias of wind speed is different from zero and statistically significant at the 99% confidence level. This result has not been discussed in the literature and warrants further investigation. If the data are instead sorted by their distance from the center of the TC, this systematic clockwise bias of wind direction is observed for locations closest to the center (figures not shown).

[19] The RMS values for low wind speeds (below 17.2 m s<sup>-1</sup>; Figures 4b and 4d) are under 2.0 m s<sup>-1</sup>, consistent with the results from previous QuikSCAT-buoy comparisons. However, in high winds (above 17.2 m s<sup>-1</sup>; Figures 4f) the RMS value is considerably larger (4.1 m s<sup>-1</sup>). This result is similar to that obtained from the QuikSCAT-buoy comparison by *Ebuchi et al.* [2002], in which obvious biases in high wind are shown in their Figure 4.

[20] Figure 5a shows the distributions of QuikSCAT-dropwindsonde wind speed differences for cases with all the rain-flagged data removed. Except for the slow-wind regime, the QuikSCAT wind has a slight negative bias of about  $-0.5$  m s<sup>-1</sup> as compared with the dropwindsonde data. The difference range (shown in the standard deviation) increases with wind speed from 1.2 m s<sup>-1</sup> in V1, 1.9 m s<sup>-1</sup> in V2, to 4.1 m s<sup>-1</sup> in V3, with a value of about 2.5 m s<sup>-1</sup> for all the matched samples. The wind speed difference in percentage is also shown Figure 5b. The mean of the difference in percentage between QuikSCAT and dropwindsonde data each wind regime is within 5%, with the value of  $-2.5\%$  for all the matched samples. A larger difference range (25%) is found in regime V1 compared with regimes V2 (15%) and V3 (20%). Overall, the standard deviation of the percentage between QuikSCAT and dropwindsonde wind speed data for all the matched samples is about 18%.

## 4. Discussion

[21] The question of why a larger difference between the QuikSCAT wind and dropwindsonde wind exists in high-

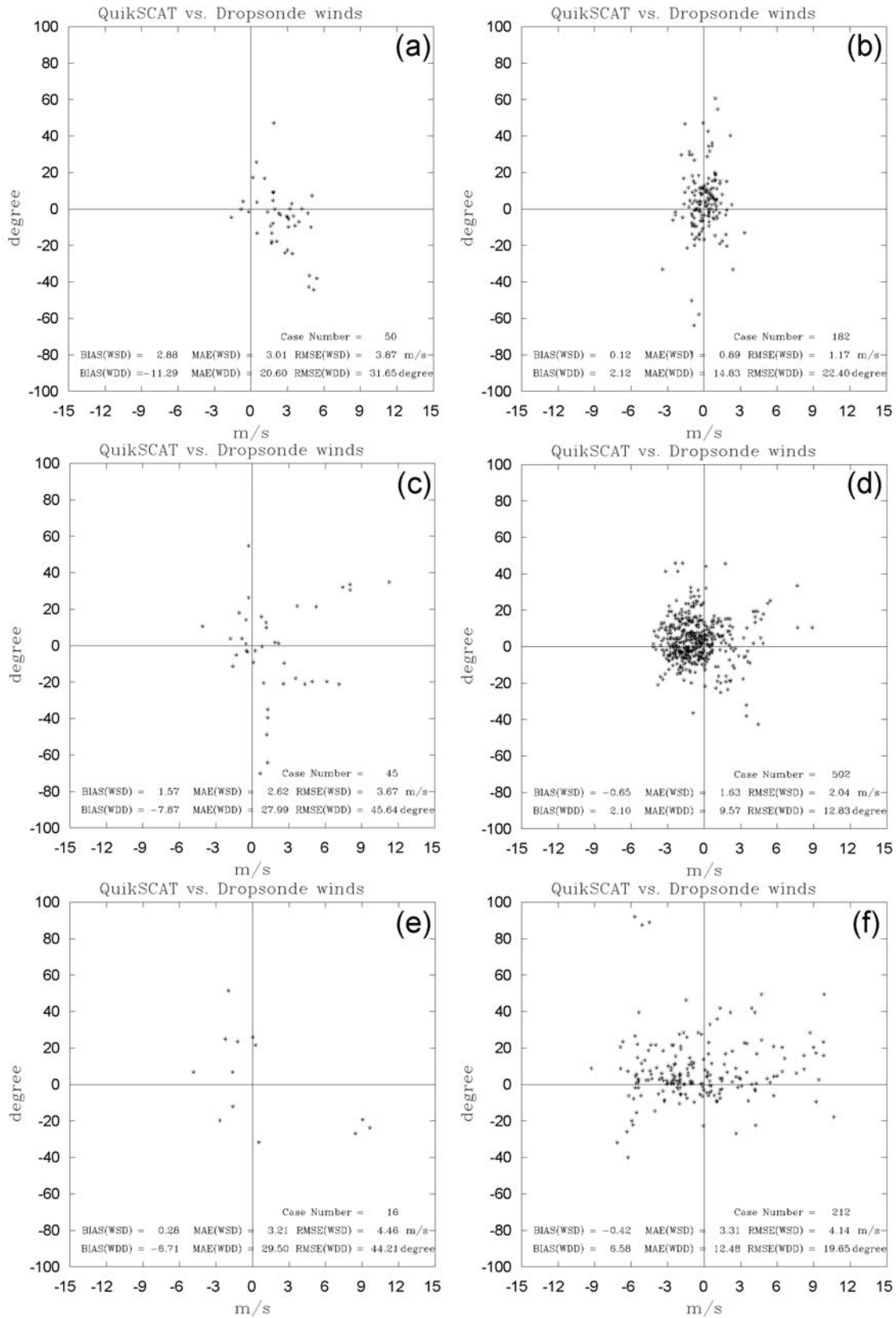


**Figure 4.** Same as Figures 3c and 3d but sorted by wind speed of the  $U_{10-M40}$  for (a, b) below  $10 \text{ m s}^{-1}$ , (c, d)  $10\text{--}17.2 \text{ m s}^{-1}$ , and (e, f) above  $17.2 \text{ m s}^{-1}$ .

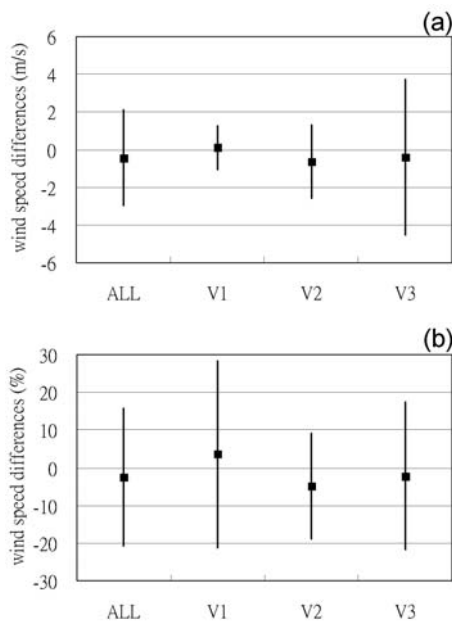


**Figure 5.** Distribution of differences between the QuikSCAT surface wind and the estimated 10 m wind for all the rain-flagged data removed and three wind regimes (V1, V2, and V3): (a) wind speed differences in  $\text{m s}^{-1}$  and (b) wind speed differences in percentage. Black squares indicate the mean of difference, and vertical lines represent the difference range within one standard deviation from the mean.

wind regimes requires further research. As an initial step, two examples (Typhoon Aere (2004) and Typhoon Bilis (2006)) are investigated, with a particular focus on the existence of large wind speed differences in areas of convection in outer spiral rainbands. As is evident in Figure 6, most of the QuikSCAT wind vectors are close to the dropwindsonde wind vectors in both cases. However, large differences exist in some dropwindsonde locations, exceeding  $10.0 \text{ m s}^{-1}$  to the northwest of Aere (Figure 6a) and to the southwest of Bilis (Figure 6c), as indicated by the red circles. Figure 6b shows the Tropical Rainfall Measuring Mission Microwave Imager (TRMM/TMI) 85 GHz brightness temperature at 0924 UTC, only 30 min before the QuikSCAT swath passed. It is clear that the area of large wind difference coincides with a heavily convective rainband of Typhoon Aere. The same result can also be inferred from the 89 GHz brightness temperature microwave image of the Aqua satellite in Bilis (Figure 6d).

[22] On the contrary, Figures 7a and 7c demonstrate the well-matched wind vectors between the QuikSCAT and dropwindsonde observations in the cases of Typhoon Longwang (2005) and Saomai (2006), in which no active outer rainbands exist around the TCs (Figures 7b and 7d). Given that the rain-flagged data have been removed from the QuikSCAT wind vectors, on the basis of the corresponding microwave images, we speculate that the current QuikSCAT processing algorithm could not effectively identify the narrow rainband structure. Although it is found that large errors exist in the rainband areas, the accuracy of QuikSCAT vectors in these areas is generally high. This finding

suggests that the QuikSCAT data are generally reliable near TCs in regions with no rain contamination.

## 5. Concluding Remarks

[23] In this study, the accuracy of QuikSCAT wind vectors in the environment of tropical cyclones (TCs) in the western North Pacific basin is determined via comparison with GPS dropwindsonde winds from DOTSTAR missions between 2003 and 2007. The dropwindsonde locations are converted to the storm-relative coordinates to the time that the QuikSCAT swath passed in order to account for the different observing times between the platforms. A regression fit is formulated between the surface to 40-m-averaged wind speed (M40) and 10 m surface wind speed ( $U_{10}$ ) in order to obtain a large database for the comparison. Comparing with the previous averaged wind methods MBL and M150 (similar with WL150), M40 method not only provides the best regression fit in wind speed, but also minimizes the wind direction errors. This result indicates the potential for using the M40 boundary layer wind to estimate  $U_{10}$  for future dropwindsonde observations.

[24] In general, on the basis of the calculation from 896 available rain-flag-removed QuikSCAT-dropwindsonde matched samples, the RMS difference between the QuikSCAT and dropwindsonde winds is  $2.6 \text{ m s}^{-1}$  (or 18%) for wind speed and  $17^\circ$  in terms of wind direction. The RMS value of wind direction is similar to that computed in previous QuikSCAT-buoy comparisons in non-TC areas, while the RMS value of wind speed is slightly larger than their findings and exceeds the satellite's design specifications ( $\pm 2 \text{ m s}^{-1}$ ). Large wind speed differences occur for higher wind regimes, and large wind direction differences occur for low-wind regimes. Nevertheless, we are able to conclude that QuikSCAT winds below tropical storm force wind strength ( $17.2 \text{ m s}^{-1}$ ) are accurate enough for the application to determine one of the key parameter of the TC structure, namely the radius of the critical wind radius of the 34 knot (tropical storm force) wind. It is important to note that QuikSCAT errors may be larger for weaker TCs where the 34 knot winds are confined to regions where heavy rain is occurring. Meanwhile, the error bound of the QuikSCAT wind estimate in high-wind regimes can be set at about  $4 \text{ m s}^{-1}$ , indicating that the QuikSCAT data still can be useful for forecasters to estimate the radius of tropical storm force winds within these error bounds, and the data could be assimilated into numerical models with new error characteristics.

[25] In the future, the work will be extended to evaluate the wind speed accuracy within the inner core of TCs, using GPS dropwindsondes deployed by the United States Air Force Reserve C-130 and Naval Research Laboratory P-3 aircraft during the Tropical Cyclone Structure (TCS-08) field experiment and T-PARC [Elsberry and Harr, 2008; C. Velden, personal communication, 2008]. The issue of correcting the rain contamination wind vector bias as shown in this work can be addressed further, making use of the originally discarded rain contaminated data as in the work of Draper and Long [2004]. A reprocessing would be necessary in order to include extra rain-flagged data, though it is beyond the scope of this paper.

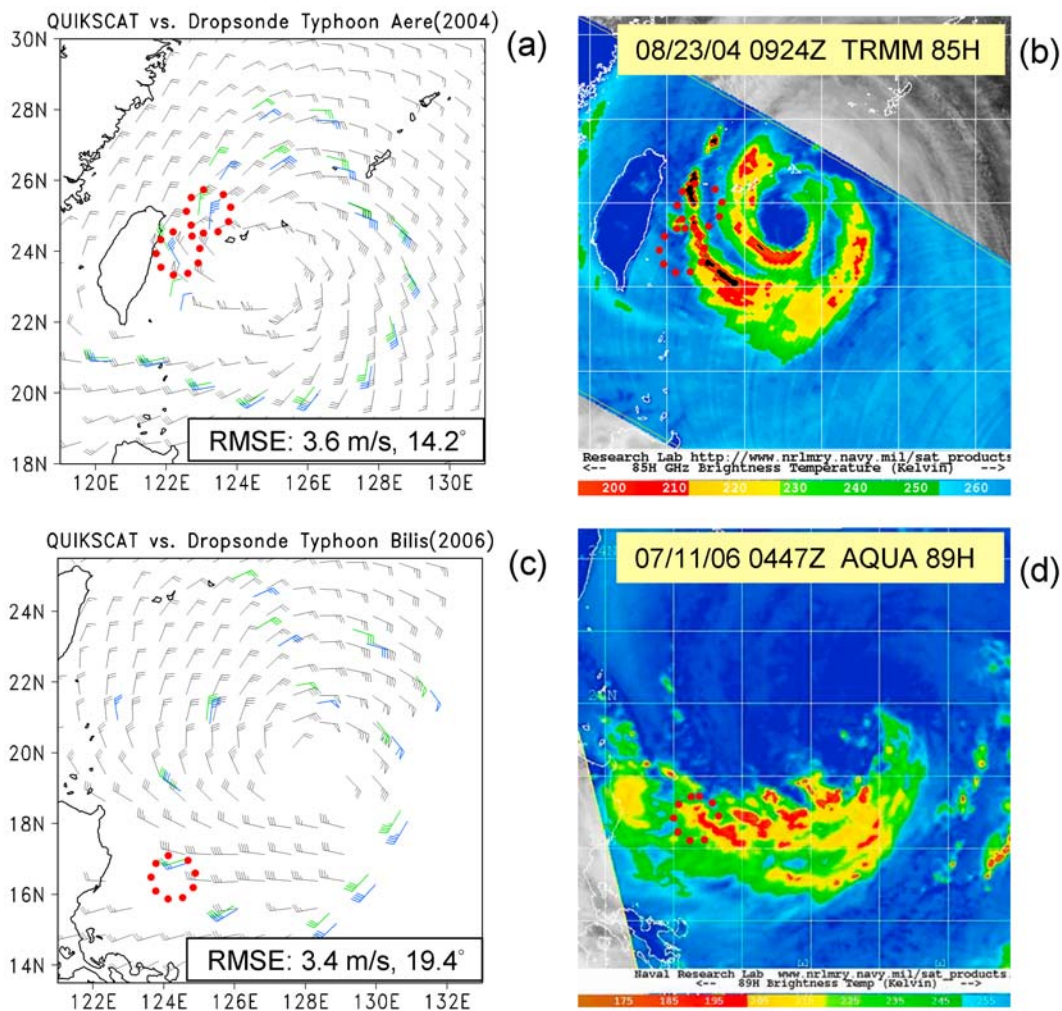


**Figure 6.** (a) Rain-flag-removed QuikSCAT surface wind (black wind barb; full barb is 10 knots) and dropwindsonde-estimated 10 m wind  $U_{10-M40}$  (original locations in green; storm-relative locations in blue) for Typhoon Aere (2004). (b) Tropical Rainfall Measuring Mission Microwave Imager (TRMM/TMI) 85 GHz brightness temperature at 0924 UTC, 23 August, for Typhoon Aere. (c) Same as Figure 6a but for the case of Typhoon Bilis (2006). (d) Same as Figure 6b but for the AQUA 89 GHz brightness temperature at 0447 UTC, 11 July, for Typhoon Bilis (from the Web site of the Naval Research Laboratory, Monterey, California).

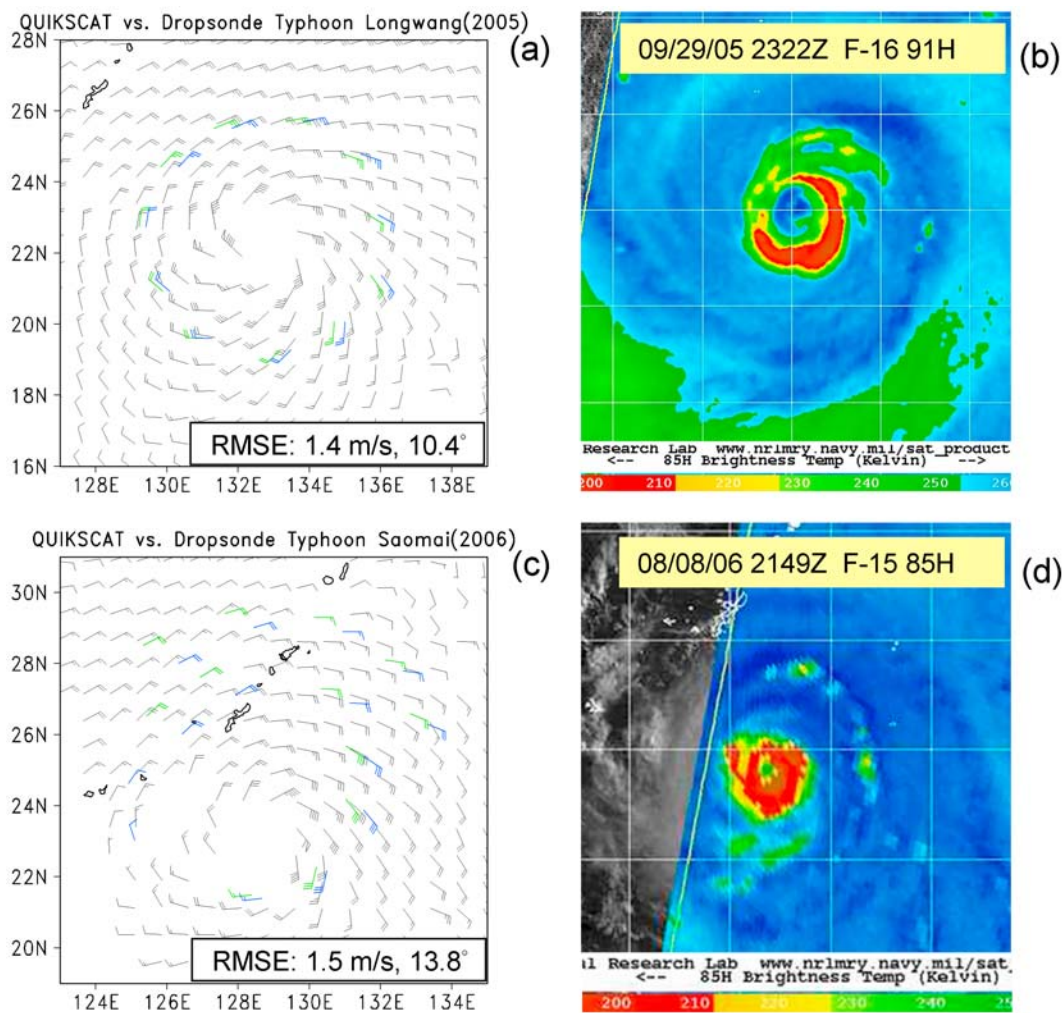


**Figure 7.** (a) Same as Figure 6a but for Typhoon Longwang (2005). (b) Microwave image for the F-16 SSMIS 91 GHz brightness temperature at 2322 UTC, 29 September, for Typhoon Longwang. (c) Same as Figure 6a but for Typhoon Saomai (2006). (d) Microwave image for the F-15 SSMIS 85 GHz brightness temperature at 2149 UTC, 8 August, for Typhoon Saomai.

[26] Another important representativeness issues when comparing the areal-averaged QuikSCAT winds and point dropwindsonde winds in the highly variable TC environment need to be addressed. A follow-up study is ongoing in which high spatial- and temporal-resolution data from numerical simulations of TCs are used to investigate the representativeness and time-averaging issues (1-min-averaged wind versus 10-min-averaged wind) of TC wind. We anticipate that this work will provide a basic knowledge on the accuracy of satellite-derived wind products, especially in TCs, for use in forecaster analysis and for initializing numerical forecast models. Moreover, the errors estimated here provide a benchmark upon which future scatterometers must improve.

[27] **Acknowledgments.** This work is supported by the National Science Council of Taiwan through grants NSC95-2119-M-002-039-MY2 and NSC-97-2111-M-034-005, the Office of Naval Research through grants N00014-05-1-0672 and N00173-08-1-G007, the National Taiwan University through grant 97R0302, and the Central Weather Bureau through grant MOTC-CWB-96-6M-02. The authors thank all DOTSTAR team members for their help in conducting the observation missions. S. J. Majumdar

acknowledges support from the NASA Ocean Vector Winds Science Team. QuikSCAT data are produced by Remote Sensing Systems and sponsored by the NASA Ocean Vector Winds Science Team (available at [www.remss.com](http://www.remss.com)).

## References

- Atlas, R., et al. (2001), The effects of marine winds from scatterometer data on weather analysis and forecasting, *Bull. Am. Meteorol. Soc.*, 82, 1965–1990, doi:10.1175/1520-0477(2001)082<1965:TEOMWF>2.3.CO;2.
- Black, P. G., R. C. Gentry, V. J. Cardone, and J. D. Hawkins (1985), Seasat microwave wind and rain observations in severe tropical and midlatitude marine storms, in *Satellite Oceanic Remote Sensing, Adv. Geophys.*, vol. 27, edited by B. Saltzman, pp. 198–279, Academic, Orlando, Fla.
- Brennan, M. J., C. C. Hennon, and R. D. Knabb (2009), The operational use of QuikSCAT ocean surface vector winds at the National Hurricane Center, *Weather Forecasting*, 24, 621–645, doi:10.1175/2008WAF2222188.1.
- Chelton, D. B., M. H. Freilich, J. M. Sienkiewicz, and J. M. Von Ahn (2006), On the use of QuikSCAT scatterometer measurements of surface winds for marine weather prediction, *Mon. Weather Rev.*, 134, 2055–2071, doi:10.1175/MWR3179.1.
- Chou, K.-H., and C.-C. Wu (2008), Development of the typhoon initialization in a mesoscale model: Combination of the bogus vortex with the dropwindsonde data in DOTSTAR, *Mon. Weather Rev.*, 136, 865–879, doi:10.1175/2007MWR2141.1.
- Draper, D. W., and D. G. Long (2004), Evaluating the effect of rain on SeaWinds scatterometer measurements, *J. Geophys. Res.*, 109, C02005, doi:10.1029/2002JC001741.

- Ebuchi, N., H. C. Graber, and M. J. Caruso (2002), Evaluation of wind vectors observed by QuikSCAT/SeaWinds using ocean buoy data, *J. Atmos. Oceanic Technol.*, *19*, 2049–2062, doi:10.1175/1520-0426(2002)019<2049:EOWVOB>2.0.CO;2.
- Elsberry, R. L., and P. A. Harr (2008), Tropical cyclone structure (TCS08) field experiment science basis, observational platforms, and strategy, *Asia Pac. J. Atmos. Sci.*, *44*, 209–231.
- Franklin, J. L., M. L. Black, and K. Valde (2003), GPS dropwindsonde wind profiles in hurricanes and their operational implications, *Weather Forecasting*, *18*, 32–44, doi:10.1175/1520-0434(2003)018<0032:GDWPIH>2.0.CO;2.
- Freilich, M. H., and R. S. Dunbar (1999), The accuracy of the NSCAT vector winds: Comparisons with National Data Buoy Center buoys, *J. Geophys. Res.*, *104*, 11,231–11,246, doi:10.1029/1998JC900091.
- Hawkins, J. D., and P. G. Black (1983), Seasat scatterometer detection of gale force winds near tropical cyclones, *J. Geophys. Res.*, *88*, 1674–1682, doi:10.1029/JC088iC03p01674.
- Hilburn, K. A., F. J. Wentz, D. K. Smith, and P. D. Ashcroft (2006), Correcting active scatterometer data for the effects of rain using passive radiometer data, *J. Appl. Meteorol. Climatol.*, *45*, 382–398, doi:10.1175/JAM2357.1.
- Hock, T. F., and J. L. Franklin (1999), The NCAR GPS dropwindsonde, *Bull. Am. Meteorol. Soc.*, *80*, 407–420, doi:10.1175/1520-0477(1999)080<0407:TNGD>2.0.CO;2.
- Hoffman, R. N., and S. M. Leidner (2005), An introduction to near real-time QuikSCAT data, *Weather Forecasting*, *20*, 476–493, doi:10.1175/WAF841.1.
- Liu, W. T., and W. Tang (1996), Equivalent neutral wind, *JPL Publ.*, 96–17, 16 pp.
- Pickett, M. H., W. Tang, L. K. Rosenfeld, and C. H. Wash (2003), QuikSCAT satellite comparison with nearshore buoy wind data off the U.S. west coast, *J. Atmos. Oceanic Technol.*, *20*, 1869–1879, doi:10.1175/1520-0426(2003)020<1869:QSCWNB>2.0.CO;2.
- Uhlhorn, E. W., P. G. Black, J. L. Franklin, M. Goodberlet, J. Carswell, and A. S. Goldstein (2007), Hurricane surface wind measurements from an operational stepped frequency microwave radiometer, *Mon. Weather Rev.*, *135*, 3070–3085, doi:10.1175/MWR3454.1.
- Von Ahn, J. M., J. M. Sienkiewicz, and P. S. Chang (2006), Operational impact of QuikSCAT winds at the NOAA Ocean Prediction Center, *Weather Forecasting*, *21*, 523–539, doi:10.1175/WAF934.1.
- Wentz, F. J., and D. K. Smith (1999), A model function for the ocean normalized radar cross section at 14 GHz derived from NSCAT observations, *J. Geophys. Res.*, *104*, 11,499–11,514, doi:10.1029/98JC02148.
- Wu, C.-C., et al. (2005), Dropwindsonde observations for typhoon surveillance near the Taiwan region (DOTSTAR): An overview, *Bull. Am. Meteorol. Soc.*, *86*, 787–790, doi:10.1175/BAMS-86-6-787.
- Wu, C.-C., K.-H. Chou, P.-H. Lin, S. D. Aberson, M. S. Peng, and T. Nakazawa (2007a), The impact of dropwindsonde data on typhoon track forecasts in DOTSTAR, *Weather Forecasting*, *22*, 1157–1176, doi:10.1175/2007WAF2006062.1.
- Wu, C.-C., J.-H. Chen, P.-H. Lin, and K.-H. Chou (2007b), Targeted observations of tropical cyclones based on the adjoint-derived sensitivity steering vector, *J. Atmos. Sci.*, *64*, 2611–2626, doi:10.1175/JAS3974.1.

---

K.-H. Chou, Department of Atmospheric Sciences, Chinese Culture University, 55, Hwa-Kang Rd., Yang-Ming-Shan, Taipei 111, Taiwan. (zcx@faculty.pccu.edu.tw)

P.-H. Lin and C.-C. Wu, Department of Atmospheric Sciences, National Taiwan University, Taipei 10617, Taiwan. (linpo@ntu.edu.tw; cwu@typhoon.as.ntu.edu.tw)

S. J. Majumdar, Division of Meteorology and Physical Oceanography, Rosenstiel School of Marine and Atmospheric Science, University of Miami, Miami, FL 33149, USA. (smajumdar@rsmas.miami.edu)